PLOS ONE

RESEARCH ARTICLE

How social learning shapes the efficacy of preventative health behaviors in an outbreak

Simon Carrignon[1]*, **R. Alexander Bentley**[1], **Matthew Silk**[2], **Nina H. Fefferman**[3,4]

1 Department of Anthropology and Center for the Dynamics of Social Complexity (DySoC), University of Tennessee, Knoxville, TN, United States of America, **2** Centre for Ecology and Conservation, University of Exeter, Exeter, United Kingdom, **3** Department of Ecology and Evolutionary Biology, University of Tennessee, Knoxville, TN, United States of America, **4** Department of Mathematics, University of Tennessee, Knoxville, TN, United States of America

* scarrign@utk.edu

Check for updates

OPEN ACCESS

Citation: Carrignon S, Bentley RA, Silk M, Fefferman NH (2022) How social learning shapes the efficacy of preventative health behaviors in an outbreak. PLoS ONE 17(1): e0262505. https://doi.org/10.1371/journal.pone.0262505

Editor: Ceyhun Eksin, Texas A&M University College Station, UNITED STATES

Received: May 20, 2021

Accepted: December 27, 2021

Published: January 11, 2022

Peer Review History: PLOS recognizes the benefits of transparency in the peer review process; therefore, we enable the publication of all of the content of peer review and author responses alongside final, published articles. The editorial history of this article is available here: https://doi.org/10.1371/journal.pone.0262505

Copyright: © 2022 Carrignon et al. This is an open access article distributed under the terms of the Creative Commons Attribution License, which permits unrestricted use, distribution, and reproduction in any medium, provided the original author and source are credited.

Data Availability Statement: All code used to generate the data is accessible here: http://github.com/simoncarrignon/slsir, compiled vignette is available here: https://simoncarrignon.github.io/

Abstract

The global pandemic of COVID-19 revealed the dynamic heterogeneity in how individuals respond to infection risks, government orders, and community-specific social norms. Here we demonstrate how both individual observation and social learning are likely to shape behavioral, and therefore epidemiological, dynamics over time. Efforts to delay and reduce infections can compromise their own success, especially when disease risk and social learning interact within sub-populations, as when people observe others who are (a) infected and/or (b) socially distancing to protect themselves from infection. Simulating socially-learning agents who observe effects of a contagious virus, our modelling results are consistent with with 2020 data on mask-wearing in the U.S. and also concur with general observations of cohort induced differences in reactions to public health recommendations. We show how shifting reliance on types of learning affect the course of an outbreak, and could therefore factor into policy-based interventions incorporating age-based cohort differences in response behavior.

Introduction

Over the course of 2020, the numbers of COVID-19 cases rose, fell, and re-surged in many Western nations. This reflected the ineffectiveness in 2020 of many Western nations to 'flatten the curve' (Fig 3), amid substantial heterogeneity of infection levels and public and government responses. Groups repeatedly gathered unprotected in 2020, despite the public health recommendations against it [1].

More understanding is needed on the acceptability of different behavioral transmission interruption strategies in context with their effectiveness [2, 3]. With important lessons for future policy, the events of 2020 reflect a familiar challenge, in that the more successful a preventative strategy is (e.g. slowing an epidemic like COVID-19), the more public demand there is to relax those successful efforts before the threat has actually passed [4–6]. This recalls the 'Icarus paradox', or failure brought about by the same strategy that led to initial success [7]. Successful preventative public health measures can facilitate the illusion that they were

slsir/vignettes/paperPLOSONE.html and pre-run simulations results here: https://osf.io/fxjh4/.

Funding: This material is based upon work supported by the NSF under award #2028710. The funders had no role in study design, data collection and analysis, decision to publish, or preparation of the manuscript.

Competing interests: The authors have declared that no competing interests exist.

unnecessary in the first place. A virus such as COVID-19 is partly invisible as it is not only contagious without obvious symptoms [8] but inadequate testing of populations [9] meant that undocumented infections likely outnumbered documented infections by an order of magnitude [8–12]. These factors (along with mixed public messaging [13]) led to underestimated risk perceptions of the virus, which for many people were overshadowed by more transparent concerns, such as financial constraints [14, 15].

While the 'Icarus paradox' has been investigated in epidemiology and community medicine studies, the complexity lies in the multiple drivers of behavioural change, including information and social learning [16–19]. Ideally, decisions would be determined by their intrinsic payoffs within their socio-ecological environment [20]. In the real world, decisions are made by people who combine observational learning, which produces noisy information, and social learning, which diffuses that information to others [21, 22].

The transparency of learning is a crucial parameter [23]; the less transparent the payoffs are, the more noise and heterogeneity enters into the behavoral dynamics [24, 25]. While humans are motivated to avoid cues associated with pathogens, through emotions such as fear or disgust [26], COVID-19 and similar viruses display few cues in asymptomatic cases [27]. If the pathogen is less visible than the behaviors of peers, avoidance behaviors will be less effective at preventing the pathogen's spread. In this situation, most people would underestimate the threat based on personal observations of infected individuals. Hence, while general social distancing would be more protective than avoiding/isolating only those individuals with obvious symptoms, its benefits may be less transparent than its economic and psychological costs [15, 28, 29].

This suggests that drivers of social distancing include two dynamic factors: observable risks and observable behaviors. The risk of infection may not become apparent until the epidemic has become widespread. At the same time, social distancing that is more visible (e.g., mask-wearing or conspicuous lack of people in public spaces) may be adopted through social influence and conformity even before its benefits are widely observed [17, 30]. Subsequently, as the true benefits become more transparent to the public, individual cost-benefit decisions can support the behavior, in place of social conformity.

Here we frame the impact of the 'Icarus paradox' as dependent on information and timing, incorporating differential age-based cohorts impacts to reflect both increased influence from peers [31] and the well-publicized age-stratified risks from infection [32]. At what point do individuals observe enough infections around them to adopt preventative behavior as their own cost/benefit decision? Before this point, in the absence of government directives, social norms may be needed to encourage protective behaviors as people are not yet observing many infections. We expect that early in an outbreak, the link between protective behaviors and being uninfected will not yet be transparent. As infection prevalence increases, and the benefits become more obvious to individuals, social learning becomes less necessary to facilitate preventative behaviors.

We believe new insights are offered by modelling the interacting effects of noisy information and social learning on behavior. We take the approach of discrete behavioral choice with social influence [33–36], where we model decisions as based on a separable combination of two components: observational and social learning. Importantly, the underlying physical contact network through which a disease might spread [37–41], which can be mitigated by physical distancing, are different than the social learning pathways of information, behaviors, or beliefs [18, 41]. Social learning can take place via a variety of media and daily communicative activities, whether physically close or distant.

Model

In order to model observational and social learning, we combine aspects of quantal response models [42, 43], which use a probabilistic (logit) choice function that allows errors in payoff estimation, with social learning of variable transparency [33, 44, 45]. Our model falls within the family of binary decision models with "positive externalities," meaning that the probability that one individual will choose a certain behavior will increase with the relative number of others choosing that same behavior [34, 46–48]. The difference with our model lies in the feedback between these externalities (social learning) with disease dynamics (observational learning).

As the dynamics are complex, we use an agent-based model (ABM) that explores two related dynamics: good protective behaviors reduce the transmission of the disease, whereas observing other infected individuals encourages (through observational learning) the adoption of protective behaviors. The aim is to tease apart the timing and impact of these different mechanisms for influencing individual behavioral choices over the course of an outbreak.

Observational learning

The individual observational learning component is governed by the payoff difference between options, based on information people receive or observe to form beliefs about their health risks [17, 18, 41, 49, 50]. For example, the perceived utility of social distancing likely increases as more illnesses are observed. In a country like the U.S., where social distancing is complicated by numerous factors both political and socioeconomic [15, 51], we see nevertheless that the number of cases predicts a measure of social distancing such as mask-wearing. As shown in Fig 1a, the relationship between mask-wearing [52] and infections per square mile (from the second week of July 2020) is sigmoidal. This is consistent with typical formulations of discrete choice theory or quantal response theory, the probability that an agent chooses choice i at time t is proportional to $e^{\kappa U_i(t)} + \epsilon_i(t)$, where κ is the transparency of choice and $U_i(t)$ is the intrinsic utility of the choice, and $\epsilon_i(t)$ is a noise term [33, 34, 42, 53].

Normalized across all choices, the sigmoid is shaped by two parameters. One parameter for this is the point at which one option has a higher utility than the other, $U_i > U_j$: we call this the 'inflection point', v. In our model, this inflection point represents the level of viral infections people perceive (assumed proportional to the number of infections in the age cohort) that signals the positive utility of social distancing in reducing infection risk. This average inflection point is a convenient modeling assumption; in reality there would be a distribution among the population as well as an 'identification problem' in detailing how a group's average behaviour influences its individuals [54, 55].

The second parameter for the observational learning component is transparency of choice, κ, which governs the steepness of the sigmoid curve: the higher the transparency of choice, the steeper the shape becomes, i.e. the smaller the variance in selecting the highest utility, U. In the real world, transparency might range from a clear, government-issued stay-home order (transparent), to seeing another person coughing, to a cacophony of conflicting media messages (non-transparent). Although these are quite different sources of information, they ultimately feed into an individual's estimate of their own risk. To a first approximation, this risk estimate from observational learning amounts to the infection rate around the person adjusted for the person's age.

We represent this as follows. Given I_a, the proportion of infected individuals in the cohort, a, the probability for an individual i to switch from 'non-adherent' status, NA, to 'adherent'

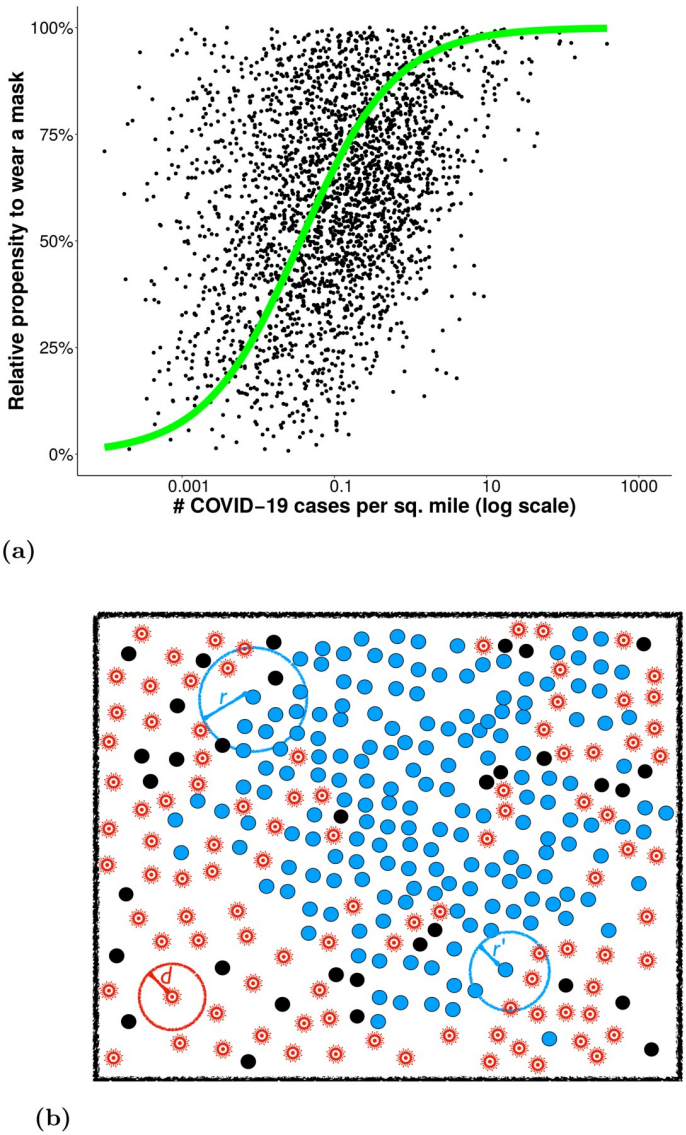

Fig 1. Model and its rationale. (a) Propensity of survey respondents in U.S. counties who 'Always' or 'Frequently' wear a mask in public during COVID-19 [52], versus confirmed infections per square mile. Data are from July 2020; each point represents a U.S. county. The green curve shows a sigmoid fit of $y = (1+ \exp[-1.6(x + 0.08)])^{-1}$. The 'propensity' on the y-axis accounts for the limited range in the county-aggregated data: about three-quarters of U.S. counties have survey results between 40% and 90% who 'always' wear masks, such that 'propensity to socially distance' measures how far each county plots between these endpoints. (b) Illustration of the agent-based model. Uninfected agents who are social distancing are colored black and agent who are not are colored blue. The circle in the lower left shows radius of infection, *d*.

https://doi.org/10.1371/journal.pone.0262505.g001

status, A, is defined as:

$$P(a, NA \rightarrow A) \sim \frac{1}{1 + e^{-\kappa(I_a - \nu)}} \tag{1}$$

where κ represents the transparency of choice—determining the steepness of the sigmoid curves—and ν defines the point at which the individual has a 50% probability to switch to adherent status, A. The influence of ν and κ, respectively, on the probability of adoption, P, is illustrated in Fig 2.

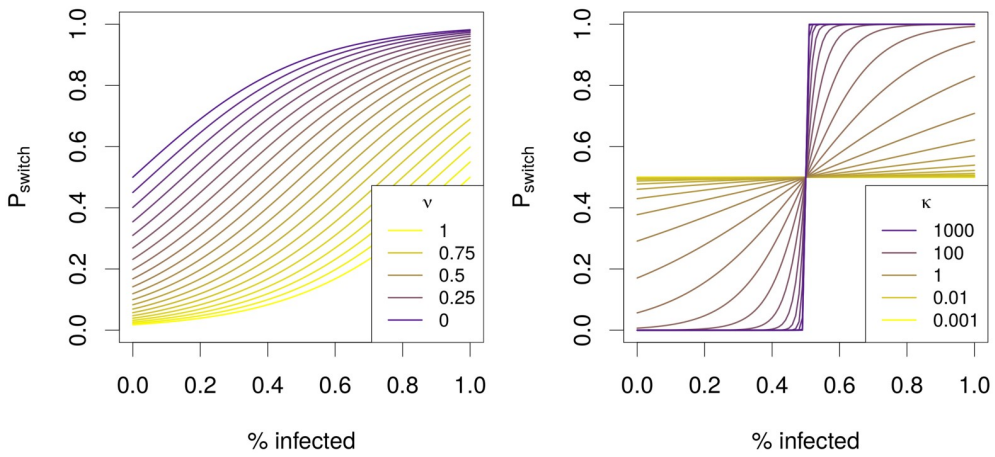

Fig 2. Illustration of the impact of transparency of choice, κ, and point of inflection, ν, on the decision curve.

https://doi.org/10.1371/journal.pone.0262505.g002

In reverse, the probability for an individual to switch back from adherent to non-adherent behavior, given the fraction of the age cohort who are not infected, $(1 - I_a)$, is:

$$P(a, A \rightarrow NA) \sim \frac{1}{1 + e^{-\kappa_r(1 - I_a - \nu_r)}} \tag{2}$$

where ν_r is inflection point for reverting to NA behavior (and can be different from ν) and κ_r the steepness of the curve use to calculate the probability of switch back to NA decision (and can also be different from κ).

Social learning

Social interactions play an important "role in mediating the spread of social contagions that impact health outcomes," [41]. Here we treat social distancing and related protective behaviors as 'simple' [41] contagions: copying what others do (e.g., wear a mask upon seeing someone else wear one). For our aggregated scale of modeling, we assume social influence operates 'as if' each person copies a currently healthy person, randomly encountered in the population, within a certain social or physical distance. The effect of the frequency of copied behaviors is stochastic, where probability of selecting option i at a time t is proportional to its current frequency or popularity, $p_{i,t}$ [33, 34, 54].

We also assume that social learning of simple behaviors (as opposed to complex skills learned over years) is biased by similarity, in that agents copy others within their cohort (a cohort could be age, political affiliation, etc). For convenience, this assumption conflates two observations, that: (a) cohorts tend already to share similar beliefs and preferences, derived from both ontogeny and broadly shared socio-economic landscape during early years of development [56–62], and (b) conformity tends to be age-dependent with cohort-biased social learning [63].

Agent-Based Model (ABM)

The ABM (Fig 1b, Algorithms 1 and 2) consists of agents who are involved in two inter-related processes, the contagion of a disease in SIR fashion [64], and the spread of protective behaviors through a combination of individual and social learning. Agents move in a grid, with a normally-distributed range of speeds. The ABM is initialized with 500 agents and one infected agent. Within this space, an infected agent can infect an uninfected agent that is not socially

distancing if within 'distance' d (Fig 1b). At the same time, agents of similar age are observing the levels of infection as well as protective behaviors, and adjusting their behaviors according to the observational and social learning rules described in Eq 1.

Algorithm 1: Main Algorithm

```
Data: N: number of of agents, t_step: number of time steps, P(b⃗): vector
      with the probability of infection for different behaviors, b d:
      the distance between two agents under which the disease can be
      transmitted, i_0: the number of initial infections, p: the proba-
      bility of observational learning, r: radius within which indi-
      vidual can learn socially κ: transparency (steepness of the
      sigmoid), ν: inflexion point of the sigmoid, κ_r: steepness of
      the reversion sigmoid, ν_r: inflexion point of the reversion
      sigmoid,
Result: A table with the SIR distribution per timestep
pop ← generatePopulation(N, x, y)
i ← pop[random(N)]
i.state ← "I" // randomly infect one individual
foreach t ∈ t_step do
  foreach a ∈ pop do
    a.move()
    X ~ U(0, 1)
    if X < p then
      // Observational Learning
      g_i ← getPropInfected(pop, a.age)
      if i.behavior = "NA" then
        p_switch ← sig(g_i, k, ν)
        X ~ U(0, 1)
        if X < p_switch then a.behavior ← "A"
      else
        p_switch ← sig(1 - g_i, k_r, ν_r)
        X ~ U(0, 1)
        if X < p_switch then a.behavior ← "NA"
      end
    else
      // Social Learning
      m ← selectModel(pop, a.age, strategy, r) // select another
      individual to copy its behavior individual within radius r
      a.behavior ← m.behavior
    end
    foreach i ∈ pop - a|dist(i, a) < d do
      X ~ U(0, 1)
      if X < P[a.behavior] then a.state ← "I"
    end
    if a.state == "I" then
      a.recovery ← a.recovery - 1
      if a.recovery < 1 then a.state ← "R"
  end
end
```

The algorithm of the ABM (Algorithms 1 and 2) relies on two main functions, one (*generatePopulation*) that generates the initial population of agents and the other (*selectModel*) that allows agents to copy the behavior of another agent, who must be both non-infected and within the same cohort, within radius r of the agent. Table 1 summarises its adjustable parameters.

Simulations were run with the parameters in Table 1, with the population initialised as described by the Algorithm 2. Some parameters were fixed (N, d_i, i_0). Initial behaviors were all

Table 1. Adjustable parameters in the agent-based simulation, with 500 agents and initialized with one infected agent.

Parameter	Description	Value
P_A	Probability a social-distancing agent (A) will infect within radius d	0.1
P_{NA}	Probability a non-social-distancing agent (NA) will infect within radius d	1
p	Probability to learn by individual observation	$U(0, 1)$
r	Radius of social learning	$U(1, 50)$
t_{step}	number of time steps	1500
d	Maximum radius for disease transmission	5
ν, ν_r	Inflection points of the learning functions	$U(0, 1)$
κ, κ_r	Transparency of choice for adopting & reverting	$10^{U(-1,\,3)}$
R	Distribution of recovery times	$R \sim U(8, 14) \times 24$
S	Distribution of the speeds of the agents	$S = \mathcal{N}(1, 0.2)$

https://doi.org/10.1371/journal.pone.0262505.t001

non-adherent to start each simulation. The speeds were sampled from a normal distribution $S \sim \mathcal{N}(1, 0.2)$ and recovery times were sampled from a uniform distribution $R \sim U(8, 14) \times 24$. The parameters were selected such that, overall, agents encounter a mean of 12 individuals per 24 time steps, such that each time step represents one hour. The recovery times in the SIR model were thus calculated to represent 8 to 14 days as a reasonable approximation for COVID-19 [65].

To explore the impact of learning on the disease outcomes over the course of an outbreak, we ran three sets of models. We first ran two baseline conditions in which individual behavior is held constant as either non-adherent (worst case scenario) or adherent (best case scenario) over the course of the simulation. We subsequently ran the models with the parameters described in Table 1 after initializing the population following Algorithm 2. In all, we ran 826,892 simulations and recorded the number of infected agents at each time step in each simulation.

Algorithm 2: Generate a population of agents

```
Data: N: number of agents, R: a uniform distribution of recovery
      times, B: a distribution of behaviors, S: a normal distribution
      of speeds, x,y: spatial limits,
Result: a table with n agents
pop = foreach a ∈ n do
  a.age ~ {.24, .09, .12, .26, .13, .16} × n // source: https://www.
  kff.org/other/state-indicator/distribution-by-age/
  a.behavior ← "NA" // by default start with everyone is Non-
  adherent
  a.position ← (rand(x), rand(y)) // random position in the grid
  a.state ← "S"
  a.recovery ~ U(8, 14) // agents have different recovery times,
  sampled between 8 and 14 days
  pop.add(a)
end
return(pop)
```

To summarize our simulations in a way that captures the 'flattening the curve', we focused on two metrics: (a) the maximum number of infected people I_{max}, and (b) the time to reach this maximum τ. As in Fig 3, the 'flat' curve has lower I_{max} and larger τ. Across all simulations, we recorded the largest and smallest maximum total infections among all the runs, as max (I_{max}) and min(I_{max}), respectively, as well as the longest and shortest times to reach the max, as max(τ) and min(τ), respectively. Since these dimensions will tend to be inversely correlated,

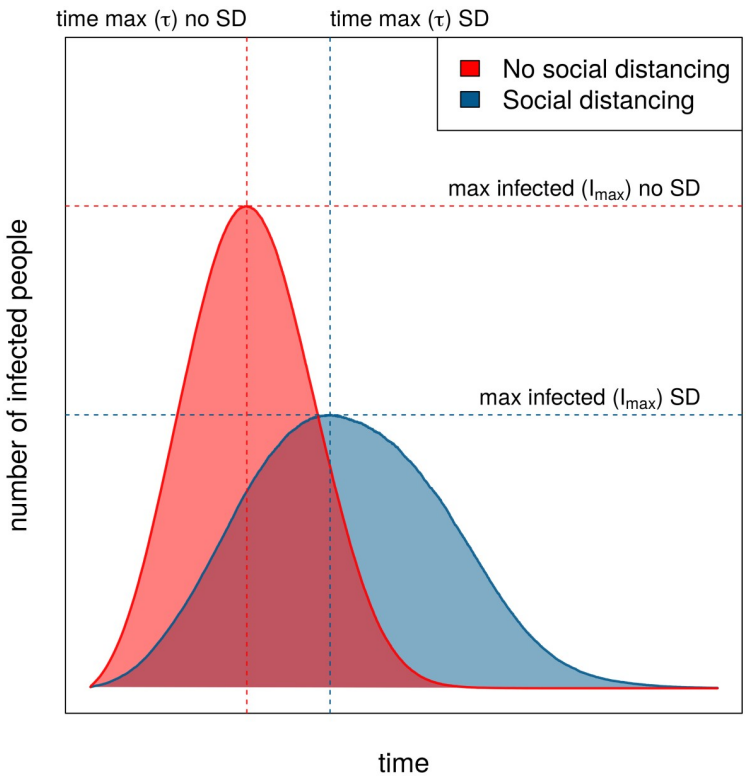

Fig 3. Illustration of the impact of social distancing on the spread of the virus.

https://doi.org/10.1371/journal.pone.0262505.g003

we defined a metric, $\delta(s)$, for a set of simulations s summarizing both:

$$\delta(s) = \frac{1}{2}\left(1 - \frac{\tau - \min(\tau)}{\Delta\tau} + \frac{I_{max} - \min(I_{max})}{\Delta I_{max}}\right) \quad (3)$$

where $\Delta I_{max} = [\max(I_{max}) - \min(I_{max})]$ and $\Delta\tau = [\max(\tau) - \min(\tau)]$, from all simulations.

Whereas our results below involve the simulation just described, we also explored three alternative scenarios, described in the S1 Text. In the first scenario individuals could copy any other individual via social learning, rather only those seen to be healthy. In the second scenario, part or all of the initial population already adhere to social distancing. The third scenario allows learning only after a certain number of time steps. The results yielded by those three alternative scenarios are given in the S1 Text but do not differ from the one presented in the next section.

Results and discussion

Our simulations produced meaningfully different outcomes that varied in the success of 'flattening the curve' (Fig 4, left). This reflects the expected patterns of outbreak curves under the impact of social distancing. Our simulations reveal multiple possible outcomes of behavioral mitigation, from 'flat' infection curves to full, unchecked outbreaks (Fig 4, right), some of which are direct illustration of the Icarus paradox.

Which learning parameters yielded the 'flattest' curve? The simulations reveal a mix of parameters underlying the best preventative outcomes. Among the simulated outbreaks in which δ were minimized—what we call the 'best' outcome—the transparency and inflection

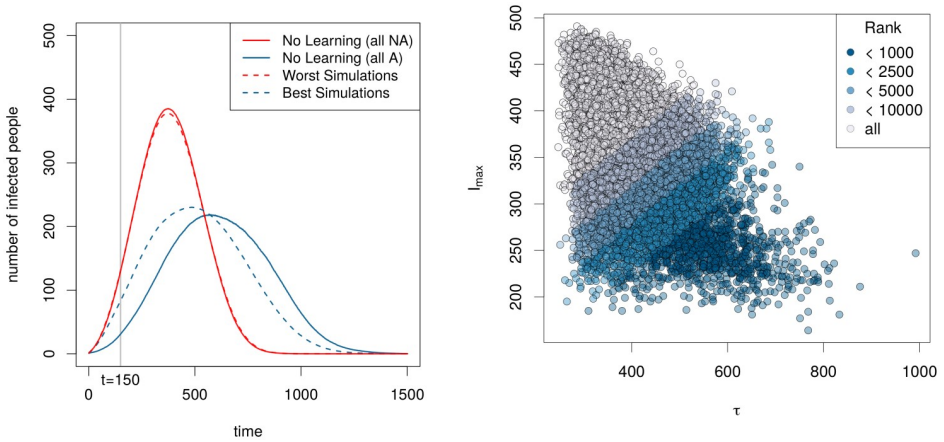

Fig 4. Left: Comparing the mean trajectories of SIR model where agents do not learn and instead continue in their initial behavior, with trajectories generated by simulations.Red curve: all agents are non-adherent to social distancing and stick to this behavior. Blue curve: all agents adhere to social distancing. Dashed red line: mean trajectory of the 1, 000 worst simulations. Blue dashed line: mean trajectory of simulations run with the parameters selected in the 1, 000 best simulations with regard to δ. Vertical gray line: status after 150 time steps. **Right**: Distribution of 826, 892 simulations given two different metrics: the maximum number of infected people (y-axis) and the time to reach this maximum (x-axis). The colors represent different class of the simulations ranked given δ, the metric defined in Eq 3.

https://doi.org/10.1371/journal.pone.0262505.g004

points (ν_r and κ_r) for reversion to non-protective behavior needed to be more constrained than the respective parameters (ν and κ) for choosing protective behavior. Fig 5 shows that the range of optimal parameters are more constrained by the end of the simulation (bottom row), which represents about two months, than they were after just 150 time steps (top row), representing approximately one week (see gray line in Fig 4). In the S1 Fig shows these joint posterior distributions in more detail.

Focusing on the end of the simulation (Fig 5, bottom row), we see different ranges of parameters yielding the 'best' (blue) and 'worst' (red) outcomes. Fig 5 shows with the joint posterior distributions of ν versus κ (adopting protective behaviors) and of ν_r versus κ_r (reversion back) on the left and right, respectively. Note particularly that the parameter regions flip-flop between adopting and reverting back. In other words, for the 'best' outcome, it is better to have low κ for adopting protective behaviors but then high κ for reverting back to non-protective behavior (see the cross-sectional distributions along the axes of each bi-variate plot in Fig 5, lower row). At the same time, for the 'best' outcome ν can be virtually any value for switching to protective behaviors, but needs to be quite high for reverting back. This exemplifies the 'Icarus' paradox: when preventive actions triggered by environmental cues bring about improvements that subsequently trigger premature relaxation of those preventative behaviors.

As a qualitative interpretation of the asymmetric effects of ν, the desired 'flat' curve is achieved through *low* transparency of choice in adopting the protective behavior, but high transparency about whether to revert back. Qualitatively the same is true of the inflection point, κ, which needs to be low in adopting the behavior but high in reverting back, in order to yield a 'flat' infection curve. These results suggest the 'best' outcomes involved a 'ratchet' effect: a low, fuzzy barrier to adopt the behavior but a high, sharp (transparent) barrier to revert back.

Our results imply that combined observational and social learning can drive successful mitigation strategies (Fig 4), even with differential, age-based disease risk. In an 'Icarus' scenario, where an initially successful strategy can lead to its own failure, the timing of these forms of learning are crucial. Those simulations yielding a flat curve generally required either low transparency of choice, low inflection point for adopting the behavior, and/or high inflection point

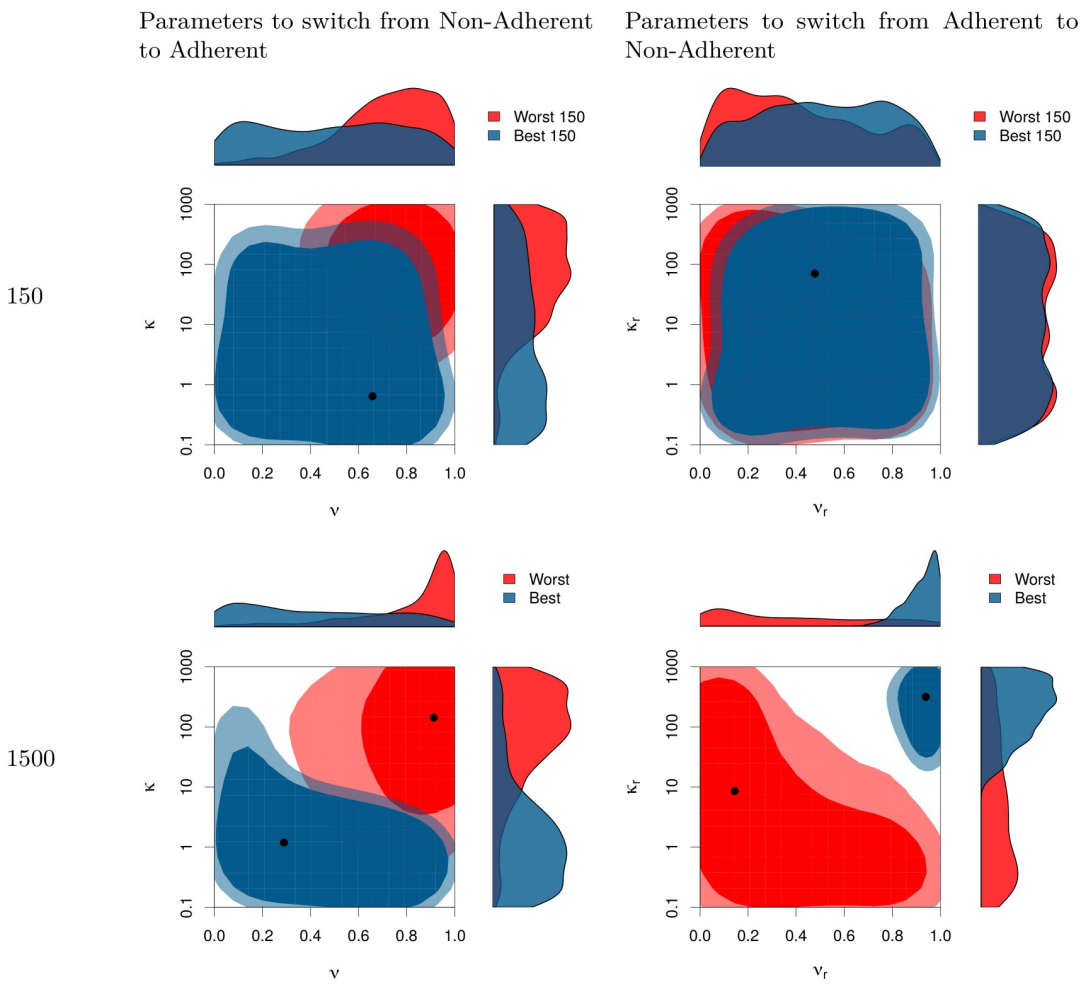

Fig 5. Joint posterior distributions for the parameters used to switch from Non-Adherent to Adherent (left column) and for the parameters used to switch back from Adherent to Non-Adherent (right column). The two-dimensional areas represent the 70% and 90% HDR (High Density Region) *i.e.*, the smallest areas within which respectively 70% and 90% of the parameters combination fall (for the mathematical definition of HDR and how they can be represented see [66]. Lighter colors represent the 90% HDR whereas darker represent the 70% HDR. The top row represents the value for those parameters that minimize (in blue) or maximize (in red) the number of infected people at time step 150. The bottom row shows the parameters that minimize (in blue) or maximize (in red) δ (as defined in Eq 3) at the end of the simulation (1500 time steps). Marginal posteriors for each parameter are drawn in the margin.

https://doi.org/10.1371/journal.pone.0262505.g005

for reversion back to non-protective behavior—in other words, a reluctance to give up the protective behavior is more important than a low threshold to acquire it (Fig 5). While it is not surprising that strong maintenance of risk-averse behaviors would protect a population, the low, fuzzy barrier to adopt these behaviours is notable and shows parallels to theory on the diffusion of innovations [48, 67, 68]. The challenge is that the risk needs to sufficiently observable to the populations that need to undertake meaningful chance. Hence protective behaviors may be not be adopted until infection rates are very high, especially if most symptomatically infected individuals are not be publicly visible (e.g., remaining at home or in hospital, or else segregated by age).

For this reason, low transparency of choice—such as poor or conflicting information —can 'jump-start' adoption of protective behaviors by stretching out the inflection into a range, such

that some individuals 'mis-estimate' infection risks as enough to trigger their decision (see Fig 5). However, this result relies on the breadth of the distribution of responses to low transparency, rather than an alternative case in which either leadership or social norms cause low transparency to lead to greater average hesitancy to take any action [69].

Social learning dynamics are crucial, as "copying recent success" is often highly adaptive [70]. If symptoms/prevalence of a disease are transparent, copying healthy individuals ('success') should increase protective behaviors. Because COVID-19 can be asymptomatic, however, infected individuals may seem healthy, such that non-protective behaviors can be copied even through a "copy success" strategy. This lack of transparency may critically compromise learning-only strategies for successful disease risk containment. By being aware of this effect, policies could be better crafted to forestall eventual rejection and thereby remain more effective in the longer term.

These effects may be heightened among young people, for whom COVID-19 infection is more frequently asymptomatic [27] and who are also socially influenced by peers in their cohort [63]. Hence, while lower fatality risk from COVID-19 may help explain why some groups of young people rejected social distancing early in the U.S. outbreak [1], another important dynamic has likely been social conformity and lack of transparency about infections among their peers.

One limitation in our simulations is that we employed a broad definition of observational learning, as agents estimate infection rates with some degree of precision (transparency). Observational learning is heterogeneous; at any given moment, each person observes different information and a different segment of the population. The real world encompasses myriad information sources, individual experiences, and biases. Also, information from media will have a different effect on decision-making than having friends and family become ill [71]. Individuals who follow stay-home protocols have different interactions than those who interact in public spaces. Taken together, these processes affect the transparency of how observably protective behaviors relate to disease risks.

These considerations are particularly relevant for mitigating pandemic spread where strong governmental control is not possible. When individual choice is the driving factor in protective behaviors, cohort effects become important since different demographic segments of societies are likely to be more initially risk-averse than others. In terms of age cohorts, for example, older individuals may be early adopters of adherent behaviors because news reports of mortality rates in older populations create a psychological burden of fear. By contrast, younger and/or more economically limited individuals may delay switching to behavioral adherence, doing so only when they feel their circumstances allow it. In such cases, the socioeconomic and demographic representation of a population may be the critical drivers in determining whether individual behaviors, guided by learning, can be relied upon to effectively achieve outbreak mitigation by adherence to social distancing.

In our models, we have also assumed that choices are rational and focused only on epidemiological risk. Human decision-making is never fully rational, especially during period of stress [72]. Further, we have here explored only one potential route of social learning, in which individuals simply copy the behaviors of perceived healthy individuals. More nuanced approaches may emphasize preferentially copying people who share your beliefs, alignment with deeply-held beliefs or values, and other social learning strategies [41, 73–75]. Similarly, we have construed frequency of contact within a spatial radius to be the only medium for social derivation of learning. In reality, of course, individuals have many means of arriving at their sense of what other people are doing, including unique personal experiences and personal choice of media, however complicated or accurate [41, 76–78]. This raises many interesting questions, such as the different effect of centralized versus diverse media, for example. Given our

parsimonious starting point, future expansion and testing of our models can address these potentially important features of social groups.

We also focused on public health measures that could be quickly adopted, in the initial case where sweeping lockdowns are not politically feasible. Our model examines the initial transient coupled dynamics directly following the introduction/emergence of a novel pathogen threat. The model proposed here focuses exclusively on the first, major wave of infections. While our contribution has been to couple the social and individual responses, we note that even in an asocial awareness model, a pandemic peak can become a prolonged plateau rather than a sharp peak, if individual transmission decreases in response to awareness of the disease at a population level [16, 79, 80].

The past two years have witnessed multiple surges of COVID-19 in many countries, including the U.S., for a diverse range of socio-political reasons [81]. Our base model presented here — focused on a single coherent, population-level response— would not, on its own, explain the observed secondary waves of COVID-19. In 2020–2021, different municipalities quickly diverged in their response to COVID-19 risks; lockdowns lasted different durations of time [79], political discourse became divisive [81], and later new strains such as Delta altered the disease epidemiology. In a mathematical model, one way to induce a second wave is to introduce a step function, representative of a centralized decision to remove lockdowns (i.e. increase spread) when public support for closure drops below a certain threshold. [82] introduce such a model, focused on centralized decisions such as school closures, that also includes social learning dynamics underlying these centralized "on-off" decisions. Since our model is based on individual, rather than centralized, decisions, this step-change instigating a second wave would not occur in our base model without more complex modifications, although this would be a valuable topic for future research. In particular, we anticipate future work where studies build on our work to investigate the various reactions that could occur as outbreaks progress. Future exploration of the model could integrate these aspects, by adding asymptomatic individuals, the apparition of new variants, more complex population structure and the possibility for recovered individuals to be infected again after a certain time. We could then explore which social learning features can mitigate subsequent waves.

Understanding how the timing and dynamics of different types of learning affect individual behavior over the course of an outbreak, as disease prevalence changes the transparency of benefits of protective behaviors, while those behaviors become more visible as they proliferate. Social learning can help boost protective behaviors, but not until the number of infections has brought about those behaviors initially through observation-driven decision making. For diseases such as COVID-19, in which age-based differences in observability and risk complicate age cohort-based learning, it may be particularly important to understand the dynamics of observability over time.

These insights translate directly into concrete recommendations for how to communicate protective health policies. Our results indicate that social influencers can be recruited from different demographic cohorts to help model protective behaviors in populations. The effect may be most poignant when certain cohorts have become jaded by or resistant to public health efforts—the point our simulations indicate can drastically shift the course of an outbreak. Further, a shift away from messages of communal support (e.g. "We're all in this together$\mathbb{H}$) to messages that more closely reflect cheer-leading (e.g. "It's working, people!") might meaningfully alter adoption and/or maintenance of protective behaviors. Making protective behaviors publicly visible among different cohorts should help to sustain those increases by social influence, and help attenuate the ensuing complacency and reversion to non-protective behavior. Policy makers who incorporate this perspective of social learning can formulate more effective

policies to anticipate the potential self-defeating effects of initially successful public protective behaviors in a disease outbreak.

Supporting information

S1 Fig. All posterior distributions. All posterior distributions for the 6 parameters used in our simulations. The white area represents the distribution of the parameters of all simulations (the priors), the blue area represents the distribution for the top 1000 simulations rank using δ while the shaded area represent the parameters of the 1000 simulations with the lowest number of infected people after 150 timesteps.Left column represents the parameters value to switch from Non-Adherent to Adherent, middle column from Adherent to Non-Adherent, and right column the paramaters that defines the probability and the radius of social learning.
(TIFF)

S2 Fig. Joint posteriors for different levels of selection. Joint posteriors of representative pair of parameters of the model for different level of what we consider as the "best" simulations. Each distribution represent the parameter distribution of simulations for which the metric δ is ranked below different level, from top to bottom: 10, 000;5, 000;2, 500;1, 000. The 2d areas represent the High Density Regions, ie the smallest regions within which falls a certain percentage of the distribution of the parameters our selected simulation. The lighter areas represent the area within which all the simulations are distributed and darker areas represent regions for smaller HDR.
(TIFF)

S1 File. Data and code. All data generated or analysed during this study are included in this published article (and its Supporting Information files). The code used to implement, run and analyse models is in R3.5 [83] and available at: https://github.com/simoncarrignon/slsir.
(TXT)

S1 Text. Different model of social learning and initial distribution. This text describes and illustrates results for 4 variants of the original model.
(PDF)

Acknowledgments

This material is based upon work supported by the NSF under award #2028710.

Author Contributions

Conceptualization: Simon Carrignon, R. Alexander Bentley, Matthew Silk, Nina H. Fefferman.

Formal analysis: Simon Carrignon, R. Alexander Bentley.

Funding acquisition: Nina H. Fefferman.

Software: Simon Carrignon.

Visualization: Simon Carrignon, Matthew Silk.

Writing – original draft: Simon Carrignon, R. Alexander Bentley, Matthew Silk, Nina H. Fefferman.

Writing – review & editing: Simon Carrignon, R. Alexander Bentley, Matthew Silk, Nina H. Fefferman.

References

1. Gharzai LA, Beeler WH, Jagsi R. Playing into Stereotypes: Engaging Millennials and Generation Z in the COVID-19 Pandemic Response. Advances in Radiation Oncology. 2020;. https://doi.org/10.1016/j.adro.2020.04.009 PMID: 32363242
2. Organization WH, et al. Coronavirus disease (COVID-2019) situation reports; 2020.
3. Bedford J, Enria D, Giesecke J, Heymann DL, Ihekweazu C, Kobinger G, et al. COVID-19: towards controlling of a pandemic. The Lancet. 2020; 395(10229):1015–1018. https://doi.org/10.1016/S0140-6736(20)30673-5 PMID: 32197103
4. Verelst F, Willem L, Beutels P. Behavioural change models for infectious disease transmission: a systematic review (2010–2015). Journal of The Royal Society Interface. 2016; 13(125):20160820. https://doi.org/10.1098/rsif.2016.0820
5. Fineberg HV. The paradox of disease prevention: celebrated in principle, resisted in practice. Jama. 2013; 310(1):85–90. https://doi.org/10.1001/jama.2013.7518 PMID: 23821092
6. Jansen VA, Stollenwerk N, Jensen HJ, Ramsay M, Edmunds W, Rhodes C, et al. Measles outbreaks in a population with declining vaccine uptake. Science. 2003; 301(5634):804–804. https://doi.org/10.1126/science.1086726 PMID: 12907792
7. Miller D. The Icarus paradox: How exceptional companies bring about their own downfall. Business Horizons. 1992; 35(1):24–35. https://doi.org/10.1016/0007-6813(92)90112-M
8. Li R, Pei S, Chen B, et al. Substantial undocumented infection facilitates the rapid dissemination of novel coronavirus (SARS-CoV2)[published online ahead of print March 16, 2020]. Science; 10.
9. Munster VJ, Koopmans M, van Doremalen N, van Riel D, de Wit E. A novel coronavirus emerging in China—key questions for impact assessment. New England Journal of Medicine. 2020; 382(8):692–694. https://doi.org/10.1056/NEJMp2000929
10. Bendavid E, Mulaney B, Sood N, Shah S, Ling E, Bromley-Dulfano R, et al. COVID-19 Antibody Seroprevalence in Santa Clara County, California. medRxiv. 2020;. https://doi.org/10.1101/2020.05.23.20111419 PMID: 32869035
11. Baud D, Qi X, Nielsen-Saines K, Musso D, Pomar L, Favre G. Real estimates of mortality following COVID-19 infection. The Lancet infectious diseases. 2020; 20(7):773. https://doi.org/10.1016/S1473-3099(20)30195-X PMID: 32171390
12. Marchant R, Samia NI, Rosen O, Tanner MA, Cripps S. Learning as we go: An examination of the statistical accuracy of COVID19 daily death count predictions. arXiv preprint arXiv:200404734. 2020;.
13. Yamey G, Gonsalves G. Donald Trump: a political determinant of covid-19; 2020.
14. Mani A, Mullainathan S, Shafir E, Zhao J. Poverty impedes cognitive function. science. 2013; 341(6149):976–980. https://doi.org/10.1126/science.1238041 PMID: 23990553
15. Trueblood J, Sussman A, O'Leary D, Holmes W. A tale of two crises: Financial constraint and perceptions of COVID-19. 2020;.
16. Funk S, Salathé M, Jansen VAA. Modelling the influence of human behaviour on the spread of infectious diseases: a review. J R Soc Interface. 2010; 106:1247–1256. https://doi.org/10.1098/rsif.2010.0142 PMID: 20504800
17. Guiteras R, Levinsohn J, Mobarak A. Encouraging sanitation investment in the developing world: A cluster-randomized trial. Science. 2015; 348:903–906. https://doi.org/10.1126/science.aaa0491 PMID: 25883316
18. Christakis NA, Fowler JH. Social contagion theory: examining dynamic social networks and human behavior. Statistics in medicine. 2013; 32(4):556–577. https://doi.org/10.1002/sim.5408 PMID: 22711416
19. Bentley RA, Earls M, O'Brien MJ. I'll have what she's having: Mapping social behavior. MIT Press; 2011.
20. Gibson MA, Lawson DW. Applying evolutionary anthropology. Evolutionary Anthropology: Issues, News, and Reviews. 2015; 24(1):3–14. https://doi.org/10.1002/evan.21432 PMID: 25684561
21. Hoppitt W, Laland KN. Social learning: an introduction to mechanisms, methods, and models. Princeton University Press; 2013.
22. Rendell L, Boyd R, Enquist M, Feldman MW, Fogarty L, Laland KN. How copying affects the amount, evenness and persistence of cultural knowledge: insights from the social learning strategies tournament. Philosophical Transactions of the Royal Society B: Biological Sciences. 2011; 366(1567):1118–1128. https://doi.org/10.1098/rstb.2010.0376 PMID: 21357234
23. Hauser OP, Rand DG, Peysakhovich A, Nowak MA. Cooperating with the future. Nature. 2014; 511(7508):220–223. https://doi.org/10.1038/nature13530 PMID: 25008530

24. Li J, Lee LF. Binary Choice under Social Interactions: An Empirical Study with and without Subjective Data on Expectations. Journal of Applied Econometrics. 2009; 24(2):257–281. https://doi.org/10.1002/jae.1035

25. Caiado CC, Brock WA, Bentley RA, O'Brien MJ. Fitness landscapes among many options under social influence. Journal of Theoretical Biology. 2016; 405:5–16. https://doi.org/10.1016/j.jtbi.2015.12.013 PMID: 26851173

26. Schrock JM, Snodgrass JJ, Sugiyama LS. Lassitude: The emotion of being sick. Evolution and Human Behavior. 2020; 41(1):44–57. https://doi.org/10.1016/j.evolhumbehav.2019.09.002

27. Kronbichler A, Kresse D, Yoon S, Lee KH, Effenberger M, Shin JI. Asymptomatic patients as a source of COVID-19 infections: A systematic review and meta-analysis. International journal of infectious diseases. 2020; 98:180–186. https://doi.org/10.1016/j.ijid.2020.06.052 PMID: 32562846

28. Maharaj S, Kleczkowski A. Controlling epidemic spread by social distancing: Do it well or not at all. BMC Public Health. 2012; 12(1):679. https://doi.org/10.1186/1471-2458-12-679 PMID: 22905965

29. Greenstone M, Nigam V. Does social distancing matter? University of Chicago, Becker Friedman Institute for Economics Working Paper. 2020;(2020-26).

30. Banerjee A, Chandrasekhar AG, Duflo E, Jackson MO. The diffusion of microfinance. Science. 2013; 341(6144):1236498. https://doi.org/10.1126/science.1236498 PMID: 23888042

31. Hogset H, Barrett CB. Social learning, social influence, and projection bias: A caution on inferences based on proxy reporting of peer behavior. Economic Development and Cultural Change. 2010; 58 (3):563–589. https://doi.org/10.1086/650424

32. Kang SJ, Jung SI. Age-related morbidity and mortality among patients with COVID-19. Infection & chemotherapy. 2020; 52(2):154. https://doi.org/10.3947/ic.2020.52.2.154 PMID: 32537961

33. Bentley RA, O'Brien MJ, Brock WA. Mapping collective behavior in the big-data era. Behavioral and Brain Sciences. 2014; 37(1):63. https://doi.org/10.1017/S0140525X13000289 PMID: 24572217

34. Brock WA, Durlauf SN. Discrete choice with social interactions. The Review of Economic Studies. 2001; 68(2):235–260. https://doi.org/10.1111/1467-937X.00168

35. Brock WA, Bentley RA, O'Brien MJ, Caiado CC. Estimating a path through a map of decision making. PloS one. 2014; 9(11). https://doi.org/10.1371/journal.pone.0111022 PMID: 25369369

36. Greene W. Econometric Analysis. ISBN: 978-0-13-139538-1; 2012.

37. Bansal S, Read J, Pourbohloul B, Meyers LA. The dynamic nature of contact networks in infectious disease epidemiology. Journal of biological dynamics. 2010; 4(5):478–489. https://doi.org/10.1080/17513758.2010.503376 PMID: 22877143

38. Donker T, Wallinga J, Grundmann H. Patient referral patterns and the spread of hospital-acquired infections through national health care networks. PLoS computational biology. 2010; 6(3). https://doi.org/10.1371/journal.pcbi.1000715 PMID: 20333236

39. Gardy JL, Johnston JC, Sui SJH, Cook VJ, Shah L, Brodkin E, et al. Whole-genome sequencing and social-network analysis of a tuberculosis outbreak. New England Journal of Medicine. 2011; 364 (8):730–739. https://doi.org/10.1056/NEJMoa1003176 PMID: 21345102

40. Meyers LA, Pourbohloul B, Newman ME, Skowronski DM, Brunham RC. Network theory and SARS: predicting outbreak diversity. Journal of theoretical biology. 2005; 232(1):71–81. https://doi.org/10.1016/j.jtbi.2004.07.026 PMID: 15498594

41. Zhang J, Centola D. Social networks and health: new developments in diffusion, online and offline. Annual Review of Sociology. 2019; 45:91–109. https://doi.org/10.1146/annurev-soc-073117-041421

42. McKelvey RD, Palfrey TR. Quantal response equilibria for normal form games. Games and economic behavior. 1995; 10(1):6–38. https://doi.org/10.1006/game.1995.1023

43. McKelvey RD, Palfrey TR. Quantal response equilibria for extensive form games. Experimental economics. 1998; 1(1):9–41. https://doi.org/10.1023/A:1009905800005

44. Brock WA, Durlauf SN. Identification of binary choice models with social interactions. Journal of Econometrics. 2007; 140(1):52–75. https://doi.org/10.1016/j.jeconom.2006.09.002

45. Blume LE, Brock WA, Durlauf SN, Jayaraman R. Linear social interactions models. Journal of Political Economy. 2015; 123(2):444–496. https://doi.org/10.1086/679496

46. Granovetter M. Threshold models of collective behavior. American journal of sociology. 1978; 83 (6):1420–1443. https://doi.org/10.1086/226707

47. Young HP. Innovation diffusion in heterogeneous populations: Contagion, social influence, and social learning. American economic review. 2009; 99(5):1899–1924. https://doi.org/10.1257/aer.99.5.1899

48. Watts DJ. A simple model of global cascades on random networks. Proceedings of the National Academy of Sciences. 2002; 99(9):5766–5771. https://doi.org/10.1073/pnas.082090499 PMID: 16578874

49. Weaver JB III, Mays D, Weaver SS, Hopkins GL, Eroğlu D, Bernhardt JM. Health information–seeking behaviors, health indicators, and health risks. American journal of public health. 2010; 100(8):1520–1525. https://doi.org/10.2105/AJPH.2009.180521

50. Funk S, Gilad E, Watkins C, Jansen VAA. The spread of awareness and its impact on epidemic outbreaks. Proc Nat Sci USA. 2009; 106:6872–6877. https://doi.org/10.1073/pnas.0810762106 PMID: 19332788

51. Ruck DJ, Bentley RA, Borycs J. Early warning of vulnerable counties in a pandemic using socio-economic variables. 2021; p. in press.

52. Katz J, Sanger-Katz M, Quealy K. A detailed map of who is wearing masks in the US. The New York Times. 2020;.

53. Arcidiacono P, Ellickson PB. Practical methods for estimation of dynamic discrete choice models. Annu Rev Econ. 2011; 3(1):363–394. https://doi.org/10.1146/annurev-economics-111809-125038

54. Brock WA, Durlauf SN. Interactions-based models. In: Handbook of econometrics. vol. 5. Elsevier; 2001. p. 3297–3380.

55. Manski CF. Identification of endogenous social effects: The reflection problem. The review of economic studies. 1993; 60(3):531–542. https://doi.org/10.2307/2298123

56. Cheung BY, Chudek M, Heine SJ. Evidence for a sensitive period for acculturation. Psychological Science. 2011; 22:147–152. https://doi.org/10.1177/0956797610394661 PMID: 21189354

57. House BR, Silk JB, Henrich J, Barrett HC, Scelza BA, Boyette AH, et al. Ontogeny of prosocial behavior across diverse societies. Proc Nat Sci USA. 2013; 110:14586–14591. https://doi.org/10.1073/pnas.1221217110 PMID: 23959869

58. Inglehart R. Changing values among western publics from 1970 to 2006. West Eur Polit. 2008; 31:130–146. https://doi.org/10.1080/01402380701834747

59. Jennings MK. Political knowledge over time and across generations. Public Opin Q. 1996; 60:228. https://doi.org/10.1086/297749

60. Ruck DJ, Bentley RA, Lawson DJ. Religious change preceded economic change in the 20th century. Science Advances. 2018; 4:eaar8680. https://doi.org/10.1126/sciadv.aar8680 PMID: 30035222

61. Ruck DJ, Bentley RA, Lawson DJ. Cultural prerequistes for socioeconomic development. Royal Society Open Science. 2020; 7:190725. https://doi.org/10.1098/rsos.190725 PMID: 32257300

62. Sears DO, Funk CL. Evidence of the long-term persistence of adults' political predispositions. Politics. 1999; 61:1–28. https://doi.org/10.2307/2647773

63. Knoll LJ, Leung JT, Foulkes L, Blakemore SJ. Age-related differences in social influence on risk perception depend on the direction of influence. J Adolesc. 2015; 60:53–63. https://doi.org/10.1016/j.adolescence.2017.07.002

64. Anderson RM, Anderson B, May RM. Infectious diseases of humans: dynamics and control. Oxford university press; 1992.

65. Russell T, Hellewell J, Abbott S, Jarvis CI, van Zandvoort K, nCov working group C, et al. Using a delay-adjusted case fatality ratio to estimate under-reporting. Euro Surveill. 2020; 25:2000256.

66. Hyndman RJ. Computing and Graphing Highest Density Regions. The American Statistician. 1996; 50(2):120–126. https://doi.org/10.2307/2684423

67. Henrich J. Cultural transmission and the diffusion of innovations: Adoption dynamics indicate that biased cultural transmission is the predominate force in behavioral change. American Anthropologist. 2001; 103(4):992–1013. https://doi.org/10.1525/aa.2001.103.4.992

68. Rogers EM. Diffusion of Innovations (4th ed.). Free Press; 1995.

69. LaVela S, Goldstein B, Etingen B, Miskevics S, Weaver F. Factors associated with H1N1 influenza vaccine receipt in a high-risk population during the 2009-2010 H1N1 influenza pandemic. Topics in spinal cord injury rehabilitation. 2012; 18(4):306–314. https://doi.org/10.1310/sci1804-306 PMID: 23459437

70. Rendell L, Boyd R, Cownden D, Enquist M, Eriksson K, Ghirlanda S, et al. Why copy others? Insights from the social learning strategies tournament. Science. 2010; 328:208–213. https://doi.org/10.1126/science.1184719 PMID: 20378813

71. Tizzoni M, Panisson A, Paolotti D, Cattuto C. The impact of news exposure on collective attention in the United States during the 2016 Zika epidemic. PLoS computational biology. 2020; 16(3):e1007633. https://doi.org/10.1371/journal.pcbi.1007633 PMID: 32163409

72. Keinan G. Decision making under stress: scanning of alternatives under controllable and uncontrollable threats. Journal of personality and social psychology. 1987; 52(3):639. https://doi.org/10.1037/0022-3514.52.3.639 PMID: 3572731

73. Weng L, Menczer F, Ahn YY. Virality prediction and community structure in social networks. Scientific reports. 2013; 3:2522. https://doi.org/10.1038/srep02522 PMID: 23982106

74. Surian D, Nguyen DQ, Kennedy G, Johnson M, Coiera E, Dunn AG. Characterizing Twitter discussions about HPV vaccines using topic modeling and community detection. Journal of medical Internet research. 2016; 18(8):e232. https://doi.org/10.2196/jmir.6045 PMID: 27573910

75. Kendal RL, Boogert NJ, Rendell L, Laland KN, Webster M, Jones PL. Social learning strategies: Bridge-building between fields. Trends in cognitive sciences. 2018; 22(7):651–665. https://doi.org/10.1016/j.tics.2018.04.003 PMID: 29759889

76. Becker J, Brackbill D, Centola D. Network dynamics of social influence in the wisdom of crowds. Proceedings of the national academy of sciences. 2017; 114(26):E5070–E5076. https://doi.org/10.1073/pnas.1615978114 PMID: 28607070

77. Centola D. Social media and the science of health behavior. Circulation. 2013; 127(21):2135–2144. https://doi.org/10.1161/CIRCULATIONAHA.112.101816 PMID: 23716382

78. Lerman K, Yan X, Wu XZ. The "majority illusion" in social networks. PloS one. 2016; 11(2). https://doi.org/10.1371/journal.pone.0147617

79. Weitz JS, Park SW, Eksin C, Dushoff J. Awareness-driven behavior changes can shift the shape of epidemics away from peaks and toward plateaus, shoulders, and oscillations. Proceedings of the National Academy of Sciences. 2020; 117(51):32764–32771. https://doi.org/10.1073/pnas.2009911117 PMID: 33262277

80. Toxvaerd FM. Equilibrium social distancing. 2020;.

81. McAdams D. The Blossoming of Economic Epidemiology. Annual Review of Economics. 2021; 13(1): 539–570. https://doi.org/10.1146/annurev-economics-082120-122900

82. Pedro SA, Ndjomatchoua FT, Jentsch P, Tchuenche JM, Anand M, Bauch CT. Conditions for a Second Wave of COVID-19 Due to Interactions Between Disease Dynamics and Social Processes. Frontiers in Physics. 2020; 8:428.

83. R Core Team. R: A Language and Environment for Statistical Computing; 2018. Available from: https://www.R-project.org/.